A Discussion of Rotating Wave Fields for Microwave Applications

Jose E. Velazco, *Member, IEEE,* and Peter H. Ceperley

***Abstract*—Traveling wave and standing wave fields are central to microwave applications. This paper discusses a third category of fields: "rotating waves" which, while ocassionally utilized in the past, are not commonly used or understood. Rotating waves are composed of a particular linear combination of standing waves, but have field profiles more similar to traveling waves. A rotating wave can be pictured as a frozen field rotating in space. An analysis is presented of rotating waves in cylindrical cavity resonators. The TM_{110} rotating mode for a cylindrical resonator is discussed in some detail.**

I. Introduction

CIRCULARLY polarized electromagnetic fields have been utilized in various applications, for example: circularly polarized antennas [1], the gyratron [2], the gyrocon [3], the magnicon [4], [5], a cyclotron converter for microwave power to direct current [4], and a self-excited microwave oscillator [4]. The gyrocon and magnicon, developed in the former Soviet Union by Budker and Karlirner, respectively, use circularly polarized fields to achieve spiraling trajectories (beam scanning) in electron beams for the generation of very high microwave power. Fig. 1 shows a schematic of the magnicon, in which three rotating mode cavities are utilized. The first two cavities modulate the beam transversely. The third cavity extracts energy from the modulated beam converting it into several megawatts of RF output power.

In this paper, we use the term "rotating waves" to describe a general class of circularly polarized electromagnetic fields, in parallel to the terms "standing waves" and "traveling waves." We start by deriving the basic equations and discussing the general properties for rotating waves. Power, energy, and angular momentum of rotating modes are then derived. The equations for rotating electromagnetic fields in cylindrical resonators are presented. Finally, we end with a more detailed discussion of the TM_{110} rotating mode in a cylindrical resonator, which has particular appeal for many microwave applications.

Manuscript received January 28, 1992; revised May 15, 1992. This work was supported by the Office of Naval Research and the Virginia Center for Innovative Technology.

J. E. Velazco is with the Microwave Research Laboratory of the Department of Electrical and Computer Engineering, George Mason University, Fairfax, VA 22030.

P. H. Ceperley is with the Department of Physics and the Microwave Research Laboratory and the Thermoacoustics Laboratory of the Department of Electric and Computer Engineering, George Mason University, Fairfax, VA 22030.

IEEE Log Number 9204491.

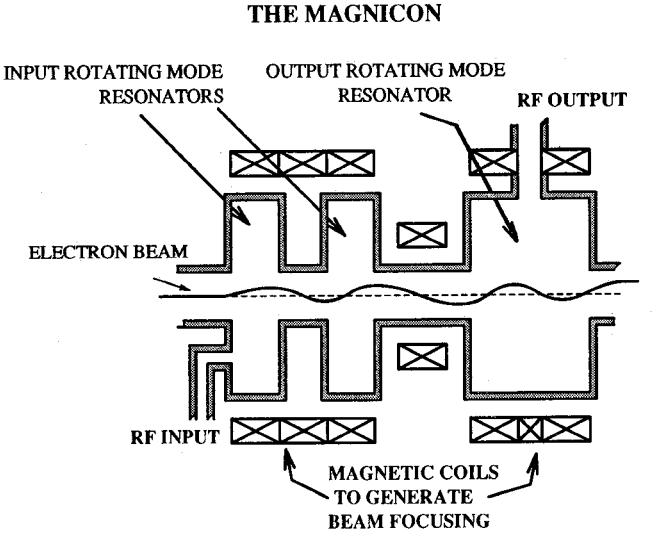

Fig. 1. Magnicon schematic.

II. Relationship Between Rotating Waves and Standing Waves

We start with a *standing wave* mode in a cylindrical cavity. For the sake of illustration, we initially consider only the z component of the electric field for a TM mode cavity of radius a and length l. The complete set of electric and magnetic field equations will be discussed in Section V. For the z component of the electric field, the field representations $E_z^{(1)}(r,\phi,z,t)$ and $E_z^{(2)}(r,\phi,z,t)$ of two identical (but shifted in the ϕ direction), mathematically independent, degenerate *standing waves* of indices m, n, and $p\,(\mathrm{TM}_{mnp})$, are given by [8]

$$\begin{aligned} E_z^{(1)}(r,\phi,z,t) &= E_0 J_m(k_c r) \\ &\quad \cdot \cos m\phi \cos k_z z \cos \omega t \\ E_z^{(2)}(r,\phi,z,t) &= E_0 J_m(k_c r) \\ &\quad \cdot \sin m\phi \cos k_z z \cos(\omega t - \delta) \end{aligned} \tag{1}$$

where $m = 0, 1, 2, 3, \cdots, J_m(k_c r)$ is an mth-order Bessel function of the first kind,

$$\omega = c(k_c^2 + k_z^2)^{1/2} \tag{2}$$

is the angular frequency, $c = (\mu\epsilon)^{-1/2}$ is the speed of light, $k_c = u_{mn}/a$ is the radial wave number, u_{mn} is the nth root of $J_m(u) = 0, k_z = p\pi/l$ is the z directed wave number, and δ is an arbitrary temporal phase shift between the two waves. The index n indicates the number of nodes (zeros) in the radial direction, and m gives the azimuthal periodicity of

the wave. The last index p gives the periodicity of the wave in the z direction. For $m = 0, \sin m\phi$ is zero everywhere making the $E_z^{(2)}(r, \phi, z, t)$ mode zero. Thus, for $m = 0$, only the $E_z^{(1)}(r, \phi, z, t)$ mode exists. It is also important that the index m is an integer so that the field at $\phi = 2\pi$ will smoothly blend with that at $\phi = 0$.

Linear combinations of the standing wave modes $E_z^{(1)}$ and $E_z^{(2)}$ for $m \geq 1$ can create rotating modes [6], [7]. For instance, adding $E_z^{(1)}$ and $E_z^{(2)}$ and setting $\delta = \pi/2$ yields a pure rotating mode

$$E_z(r, \phi, z, t) = E_0 J_m(k_c r) \cos k_z z \cos(\omega t - m\phi), \quad m = 0, 1, 2, 3 \cdots . \tag{3}$$

Subtracting $E_z^{(1)}$ and $E_z^{(2)}$ in (1) also results in rotating waves which can be expressed by (3) considering now $m = -1, -2, -3 \cdots$ (i.e., the m in (3) equals $-m$ of (1) when we substract). Thus, in either case (adding or subtracting), (3) represents rotating modes for $m = \cdots -3, -2, -1, 0, 1, 2, 3 \cdots$. A mode with positive m value will rotate counterclockwise (positive ϕ direction), while its *degenerate* counterpart of equal magnitude but negative m value will rotate clockwise (negative ϕ direction). An added benefit of (3) is that it assigns only one mode to each combination of m and n, thus eliminating the need for the somewhat odd, doubly degenerate modes for $m \geq 1$ as in (1). Equation (3) can also be expressed in complex form as

$$E_z(r, \phi, z, t) = E_0 J_m(k_c r) \cos k_z z e^{j(\omega t - m\phi)}. \tag{4}$$

Equations (3) and (4) represent a pure rotating wave. The $\cos(\omega t - m\phi)$ term in (3) is similar to a $\cos(\omega t - kx)$ term in a traveling wave, with the only difference being that in this case the waves are traveling in the ϕ direction, around in circles. They appear as traveling waves chasing their tails. Fig. 2 shows the z electric wave field in the TM_{520} mode. One can easily see the periodicity in the ϕ direction, $m = 5$ in this case, and the number of zeros in the radial direction, $n = 2$. The snapshot of a standing wave for this mode would not differ from the one of a rotating wave. It is the dynamics of the wave crests, as indicated by the arrows on the figure, that distinguish these as rotating waves. Standing waves appear to vibrate between fixed nodal lines and continually change their shape, i.e., have time dependence. A rotating wave, on the other hand, has a constant but moving field profile, similar to that of a traveling wave. Nevertheless, rotating waves *do* have discrete resonant frequencies with integer indices [m, n, and p in (2)] similar to that of standing waves. Thus, rotating waves have properties of both standing and traveling waves.

In order to calculate the velocity with which this wave travels in the ϕ direction, we need to follow a feature, such as a node or a maximum, as the wave propagates. Such a feature is defined by a particular value C of the argument of the last cos in (3) or value of the argument of the exponential of (4), i.e., $C = \omega t - m\phi = 0, 2\pi, 4\pi$, etc., for the wave peaks, or $\pi/2, 3\pi/2$, etc., for the nodes, and $\pi, 3\pi$, etc., for the valleys. In general, for any particular feature

$$\omega t - m\phi = C \tag{5}$$

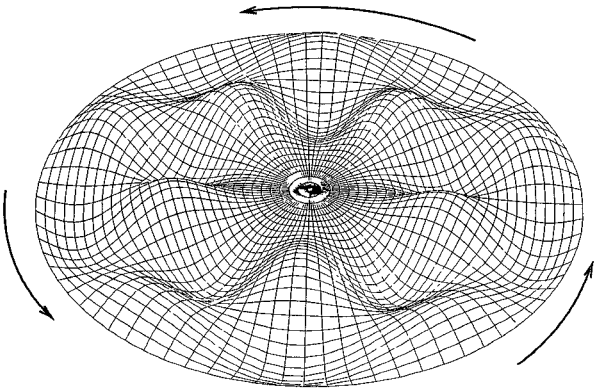

Fig. 2. Surface plot of E_z in rotating TM_{520} mode.

where C is a constant. After applying derivatives to (5), we can obtain

$$m\, d\phi = \omega\, dt \tag{6}$$

which can be rearranged to yield

$$\frac{d\phi}{dt} = \frac{\omega}{m}. \tag{7}$$

This expression indicates that the angular velocity of the rotating wave $\omega_{\text{rot}} \equiv d\phi/dt$ equals the RF angular frequency ω divided by the azimuthal index m. For example, for $m = 4$, the wave would be rotating at an angular velocity equal to a quarter of the RF angular frequency, $\omega_{\text{rot}} = \omega/4$. This is of special importance in high-frequency microwave applications. In devices like the magnicon, in order to obtain synchronism between fields and particles, the cyclotron frequency of the electrons Ω_c is matched to the rotating frequency of the cavities' fields, i.e., $\Omega_c = 2\omega_{\text{rot}}$ for the input cavities, $\Omega_c = \omega_{\text{rot}}$ for the output cavity. The cyclotron frequency is directly dependent on the axial magnetic field B_z applied on the particles, $\Omega_c = eB_z/m_o$ [9]. Here e and m_o are the electron charge and mass, respectively. For high-frequency applications, very strong magnetic field systems would be necessary, which besides becoming large and expensive, could lead to potential problems such as overheating or beam pinch-off, among others. For a higher order mode cavity ($|m| > 1$), the rotating frequency of the fields will be smaller than ω by a factor of $1/m$, hence relaxing the need for a strong axial magnetic field. Other potential applications may be encountered that also utilize the fact that while the cavity is resonating at ω, its fields are rotating at ω/m.

III. Energy, Power, and Angular Momentum in Rotating Waves

In an electromagnetic rotating wave resonance, the field components rotate in the ϕ direction. Moreover, the electric and magnetic fields, whose time and ϕ dependence are of the form $e^{j(\omega t - m\phi)}$, are "in phase" both in time and in position. This will be explained in more detail in Section V-A. This results in there being a ϕ directed time averaged Poynting vector P_ϕ produced by these fields and given by

$$P_\phi = \frac{1}{2} \operatorname{Re}(\boldsymbol{E} \times \boldsymbol{H}^*)_\phi$$

where $\boldsymbol{E}$ and $\boldsymbol{H}$ are the complex representation of the electric and magnetic field components transverse to the direction of motion ϕ.

A characteristic parameter of rotational motion is the angular momentum L_z. The z directed angular momentum density l_z equals the cylindrical radius r times the linear momentum density $P\phi/c^2$ [10]–[12], where c is the free-space phase velocity of the electromagnetic radiation. If we integrate l_z over the volume of the resonator, we obtain an expression for the angular momentum L_z as follows:

$$L_z = \frac{1}{c^2}\int_V \frac{1}{2}\operatorname{Re}(\boldsymbol{E}\times\boldsymbol{H}^*)_\phi r\,dV. \tag{8}$$

The Maxwell equation $j\omega\boldsymbol{E} = c^2\mu\nabla\times\boldsymbol{H}$ yields

$$L_z = -\frac{\mu}{\omega}\int_V \frac{1}{2}\operatorname{Re}[j((\nabla\times\boldsymbol{H})\times\boldsymbol{H}^*)_\phi]r\,dV.$$

Substituting specific components of the vectors in *cylindrical coordinates*, we have

$$L_z = -\frac{\mu}{\omega}\int_V \frac{1}{2}\operatorname{Re} j\left\{\left[\frac{1}{r}\frac{\partial(rH_\phi)}{\partial r} - \frac{1}{r}\frac{\partial H_r}{\partial\phi}\right]\cdot H_r^* - \left[\frac{1}{r}\frac{\partial H_z}{\partial\phi} - \frac{\partial H_\phi}{\partial z}\right]H_z^*\right\} r\,dV. \tag{9}$$

Utilizing the fact that the ϕ dependence of the fields is of the form $e^{-jm\phi}$, we have for (9)

$$L_z = \frac{\mu}{\omega}\int_V \left[\frac{1}{2}m|\boldsymbol{H}|^2 + \frac{1}{2}\operatorname{Re}(j\nabla(rH_\phi)\cdot\boldsymbol{H}^*)\right]dV. \tag{10}$$

Replacing $U_B = (\mu/4)\int_v |\boldsymbol{H}|^2\,dV$ for the magnetic energy [13] and expanding the term on the right, we have

$$L_z = 2\frac{m}{\omega}U_B + \frac{\mu}{\omega}\int_V \frac{1}{2}\operatorname{Re}\left[j\nabla\cdot(rH_\phi\boldsymbol{H}*) - j\left(\underbrace{\nabla\cdot\boldsymbol{H}^*}_{=0}\right)rH_\phi\right]dV \tag{11}$$

where the foremost right expression is zero from the Maxwell equation $\mu\nabla\cdot\boldsymbol{H} = 0$. Now applying the divergence theorem on the expression at the center, we obtain

$$L_z = 2\frac{m}{\omega}U_B + \frac{\mu}{2\omega}\underbrace{\operatorname{Re}\left(j\oint_S rH_\phi\boldsymbol{H}^*\cdot d\boldsymbol{S}\right)}_{=0}. \tag{12}$$

The expression on the right is zero by the fact that $\boldsymbol{H}$ at the resonator wall is perpendicular to the wall surface vector $\boldsymbol{S}$.

Finally, observing that the total magnetic energy U_B comprises half the total field energy U, we obtain a final expression for the angular momentum

$$L_z = \frac{mU}{\omega}. \tag{13}$$

It is interesting to note that while the fields rotate at $\omega_{\text{rot}} = \omega/m$, i.e., rotate slower for larger m values, the angular momentum L_z, which is proportional to m, increases for larger m values.

TABLE I
THE nth ROOTS OF $J_m(u)$

m / n	0	1	2	3
1	2.405	3.832	5.136	6.380
2	5.520	7.016	8.417	9.761
3	8.654	10.173	11.620	13.015
4	11.792	13.324	14.796	16.223

TABLE II
THE nth ROOTS OF $J'_m(u)$

m / n	0	1	2	3
1	3.832	1.841	3.054	4.201
2	7.016	5.331	6.706	8.015
3	10.173	8.536	9.969	11.346
4	13.324	11.706	13.170	14.587

In the output cavity of the magnicon, most of the gyrating beam energy is given to the cavity fields which result in an associated loss in the electrons' momentum. Clearly, by the conservation of momentum, the fields must gain an equivalent amount (L_z must increase accordingly) which in turn translates into the enhancement of the fields energy U.

IV. Resonant Frequencies of Rotating Waves

From the derivations in Section II, we see that the resonant frequencies of the rotating modes are same as the resonant frequencies of standing waves modes [14], given in (2),

$$\omega_{mnp} = c[k_c^2 + k_z^2]^{1/2}. \tag{14}$$

Substituting the expression for k_c and k_z, we obtain

$$\omega_{mnp} = c\sqrt{\left(\frac{u_{mn}}{a}\right)^2 + \left(\frac{p\pi}{l}\right)^2}. \tag{15}$$

Similarly, the resonant frequencies for the TE_{mnp} mode are given by

$$\omega_{mnp} = c\sqrt{\left(\frac{u'_{mn}}{a}\right)^2 + \left(\frac{p\pi}{l}\right)^2} \tag{16}$$

where u'_{mn} is the nth root of the $J'_m(u) \equiv dJ_m(u)/du = 0$. Tables I and II show the nth roots of $J_m(u)$ and $J'_m(u)$, the mth- order Bessel functions of the first kind, for different values of m and n for the various rotating modes of waves in a cylindrical guide. The frequency is a function of the index numbers n and p, and the *absolute value* of m. For $|m| \geq 1$, the $+m$ and $-m$ modes are degenerate, as mentioned in Section II.

V. Rotating Wave Fields in Cylindrical Resonators

The standard equations for the electromagnetic standing wave modes TM_{mnp} in cylindrical resonators are [8]

$$E_z(r,\phi,z,t) = E_0 J_m(k_c r)\cos k_z z \cdot \cos(m\phi)\cos\omega t \tag{17}$$

$$E_r(r,\phi,z,t) = -\frac{E_0}{k_c}\left(\frac{p\pi}{l}\right)J'_m(k_c r)\sin k_z z \cdot \cos m\phi \cos \omega t \quad (18)$$

$$E_\phi(r,\phi,z,t) = \frac{E_0}{k_c^2}\left(\frac{m}{r}\right)\left(\frac{p\pi}{l}\right)J_m(k_c r)\sin k_z z \cdot \sin m\phi \cos \omega t \quad (19)$$

$$H_r(r,\phi,z,t) = \frac{\omega\epsilon E_0}{k_c^2}\left(\frac{m}{r}\right)J_m(k_c r)\cos k_z z \cdot \sin m\phi \sin \omega t \quad (20)$$

$$H_\phi(r,\phi,z,t) = \frac{\omega\epsilon E_0}{k_c}J'_m(k_c r)\cos k_c z \cos m\phi \sin \omega t \quad (21)$$

$$H_z(r,\phi,z,t) = 0. \quad (22)$$

By shifting phases (both in the angle ϕ and in time), and adding these as we did in Section II, we find the complete electromagnetic fields for the rotating wave modes in a TM_{mnp} cylindrical resonator:

$$E_z(r,\phi,z,t) = E_0 J_m(k_c r)\cos k_z z \cos(\omega t - m\phi) \quad (23)$$

$$E_r(r,\phi,z,t) = -\frac{E_0}{k_c}\left(\frac{p\pi}{l}\right)J'_m(k_c r)\sin k_z z \cdot \cos(\omega t - m\phi) \quad (24)$$

$$E_\phi(r,\phi,z,t) = \frac{E_0}{k_c^2}\left(\frac{m}{r}\right)\left(\frac{p\pi}{l}\right)J_m(k_c r)\sin k_z z \cdot \sin(\omega t - m\phi) \quad (25)$$

$$H_r(r,\phi,z,t) = \frac{\omega\epsilon E_0}{k_c^2}\left(\frac{m}{r}\right)J_m(k_c r)\cos k_z z \cdot \cos(\omega t - m\phi) \quad (26)$$

$$H_\phi(r,\phi,z,t) = \frac{\omega\epsilon E_0}{k_c}J'_m(k_c r)\cos k_z z \sin(\omega t - m\phi) \quad (27)$$

$$H_z(r,\phi,z,t) = 0. \quad (28)$$

where $m = \cdots -3,-2,-1,0,1,2,3,\cdots$, and $J'_m \equiv (d/dk_c r)[J_m(k_c r)] = [(m/k_c r)J_m(k_c r) - J_{m+1}(k_c r)]$ [15]. A discussion of the characteristics of and the difference between the standing wave and rotating wave representation of these fields is presented below for the TM_{110} mode case.

A. TM_{110} *Cylindrical Resonator Case*

For a TM_{110} mode cylindrical cavity, the standing wave representation (17)–(22) reduces to

$$E_z(r,\phi,t) = E_0 J_1(k_c r)\cos\phi\cos\omega t \quad (29)$$

$$H_r(r,\phi,t) = \frac{\omega\epsilon E_0}{k_c^2 r}J_1(k_c r)\sin\phi\sin\omega t \quad (30)$$

$$H_\phi(r,\phi,t) = \frac{\omega\epsilon E_0}{k_c}J'_1(k_c r)\cos\phi\sin\omega t \quad (31)$$

and the rotating representation (23)–(28) to

$$E_z(r,\phi,t) = E_0 J_1(k_c r)\cos(\omega t - \phi) \quad (32)$$

$$H_r(r,\phi,t) = \frac{\omega\epsilon E_0}{k_c^2 r}J_1(k_c r)\cos(\omega t - \phi) \quad (33)$$

$$H_\phi(r,\phi,t) = \frac{\omega\epsilon E_0}{k_c}J'_1(k_c r)\sin(\omega t - \phi) \quad (34)$$

where $J'_1 = [(J_1(k_c r)/k_c r) - J_2(k_c r)]$. The plots of J_m are shown in Fig. 3 for $m = 0,1,2$.

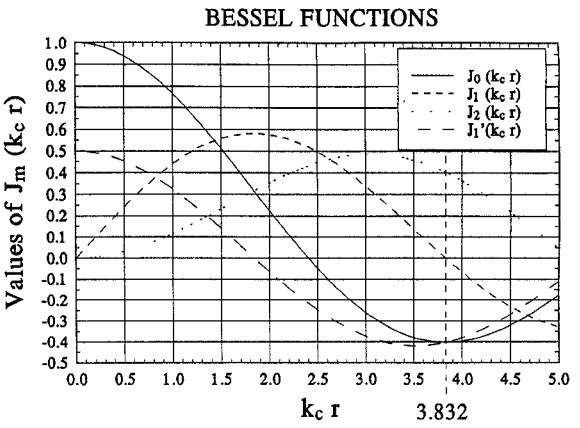

Fig. 3. Bessel function plots.

For *standing waves*, the fields (29)–(31) cycle between being totally magnetic and being totally electric; so that when the magnetic field is maximum, the electric field is zero, and vice versa. The magnetic lines wrap around in closed curves in both halves of the cavity, reinforcing each other at the center as shown in Fig. 4(a). The electric field lines go perpendicular (to the plane of the magnetic field lines) through the center of the magnetic field curves where the magnetic field is minimum. For *rotating waves* (32)–(34), the electric and magnetic fields are both always present (instead of cycling), and the field patterns of each are unchanging, but rotating in the ϕ direction. The profile of the electric field lines of a rotating wave is the same as that in the standing wave case. Also, the profile of the magnetic field lines is the same as in the standing wave case. However, the electric and magnetic field profiles have a different relative orientation in the rotating wave case as compared to the standing wave case. As shown in Fig. 4(b), the electric field profile is rotated by 90° relative to the magnetic field profile when compared to the standing wave case shown in Fig. 4(a). Considering fields off the resonator axis (at some radial coordinate value r), in the *standing wave* case, the electric field peaks at a different ϕ coordinate value than the magnetic field. In the rotating wave case, they peak at the same ϕ coordinate value and same time, creating a strong circulating Poynting vector $P_\phi = (1/2)\,\mathrm{Re}\,(E_z \times H_r^*)$ with the associated angular momentum discussed in Section III. In contrast, in the standing wave case, the Poynting vector averaged over an RF cycle is everywhere zero. Fig. 5(a) shows a snapshot surface plot for the rotating electric field E_z of the TM_{110} cavity. From (32) and (33) we see that the radial magnetic field component H_r is proportional to E_z, so its snapshot surface plot would look the same as Fig. 5(a). Note also that, off-axis, the fields E_z and H_r being proportional to each other, peak simultaneously (in time and position) as they rotate, creating a rotating Poynting vector as stated above. As is well known, in a cavity at resonance (in a standing wave mode), the stored energy U is *constant* and oscillates between electric and magnetic forms [16]. That is to say, because the electric and magnetic fields in the standing wave case are 90° out of phase, the electric energy $U_E \propto |E|^2$ peaks when the magnetic energy $U_H \propto |H|^2$ is zero, and vice versa.

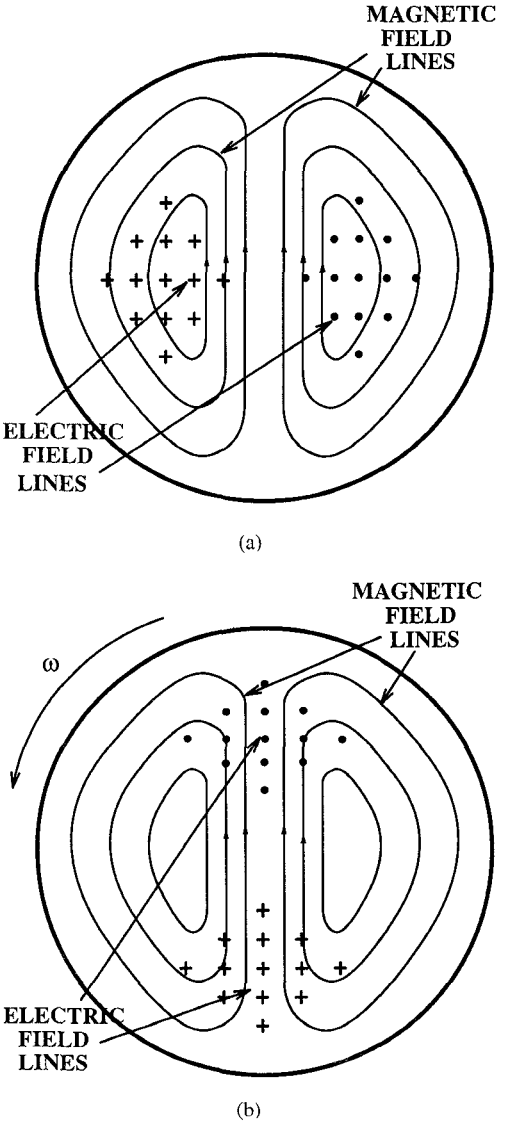

Fig. 4. (a) Electromagnetic field lines for standing wave TM_{110} mode in a cylindrical resonator. (b) Electromagnetic field lines for rotating wave TM_{110} mode.

In a rotating wave mode, the fields rotate in the ϕ direction, keeping their amplitude constant as they travel. Therefore, the total electric energy and the magnetic energy will both be constant in time and each equal to half the total stored energy:

$$U_E(t) = U_H(t) = \frac{1}{2}U(t).$$

To demonstrate the previous statement, we calculate the electric stored energy of a TM_{110} rotating wave resonator as follows:

$$U_E = \int_V \frac{\epsilon}{2}|E_z|^2\,dV = \frac{\epsilon}{2}\int_0^l\int_0^{2\pi}\int_0^a |E_0 J_1(k_c r)\cos(\phi-\omega t)|^2 r\,dr\,d\phi\,dz \quad (35)$$

and the magnetic stored energy

$$U_H = \int_V \frac{\mu}{2}[|H_r|^2 + |H_\phi|^2]\,dV$$

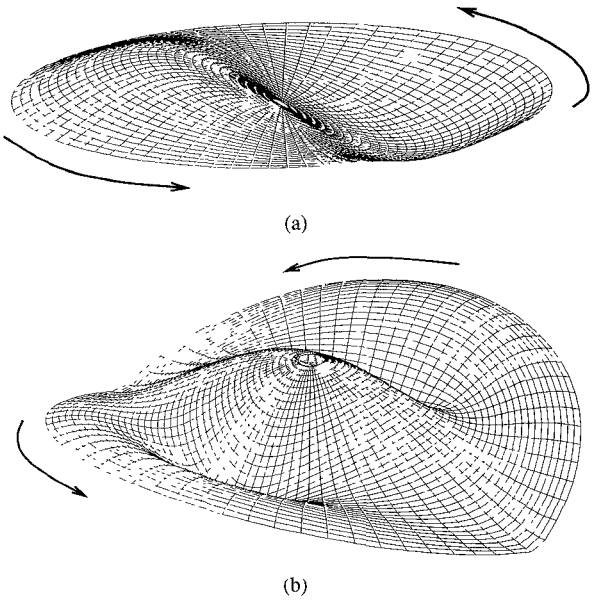

Fig. 5. (a) Surface plot of electric field E_z for rotating TM_{110} mode cavity. A similar plot of H_r will have exactly the same shape. (b) Surface plot of total H field ($\sqrt{H_\phi^2 + H_r^2}$) for a rotating TM_{110} mode in a cylindrical resonator.

$$= \frac{\mu}{2}\int_0^l\int_0^{2\pi}\int_0^a \left[\left|\frac{\omega\epsilon E_0}{k_c^2 r}J_1(k_c r)\cos(\phi-\omega t)\right|^2 + \left|\frac{\omega\epsilon E_0}{k_c}J_1'(k_c r)\sin(\phi-\omega t)\right|^2\right] r\,dr\,d\phi\,dz. \quad (36)$$

As expected, (35) and (36) give the same answer [17]

$$U_E = U_H = \frac{1}{4}\pi\epsilon a^2 l J_0^2(u_{11})E_0^2. \quad (37)$$

Thus, in the rotating wave case, the electric and magnetic stored energies are identical to each other, and are constant or *time independent.*

In both standing wave and rotating wave modes, the coefficient of the electric field E_0 can be found from (37). Substituting $U = P_{in}Q/\omega$ [18], we have

$$E_0 = \frac{2}{aJ_0(u_{11})}\sqrt{\frac{Q}{\omega\pi\epsilon l}\left(\frac{P_{in}}{2}\right)} \quad (38)$$

where Q is the quality factor of the cavity and P_{in} is the power fed to the cavity. So by (32), the electric field magnitude at any r value is $E_0 J_1(k_c r)$, and the maximum value in the cavity occurs at $k_c r = 1.841$ and equals $0.582E_0$. The magnetic field magnitude then is given by (33) and (34). Thus, for a given cavity, (38) allows us to determine the peak (and ever-present but moving) electric and magnetic field magnitudes inside of the cavity.

We calculate the resonant frequency of the TM_{110} modes by examining the boundary conditions. The boundary conditions for the electric field component require that $E_z = 0$ for $r = a$. Table I yields for $m = n = 1, u_{11} = 3.832$ (i.e., for $k_c r = 3.832, J_1(k_c r) = 0$ as shown in Fig. 3). Equation (14) gives the resonant frequency

$$\omega_{110} = c\frac{u_{11}}{a} = 3.832\frac{c}{a}. \quad (39)$$

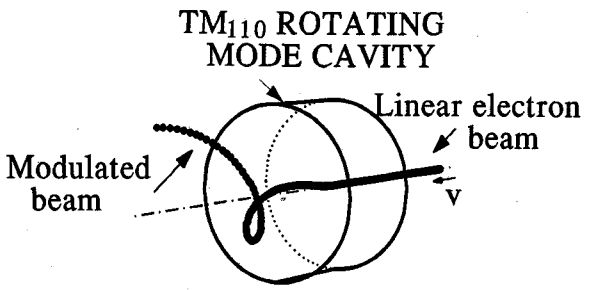

Fig. 6. Snapshot of an electron beam going through a TM_{110} cavity.

Equation (7) indicates that the fields within this cavity will rotate at the angular velocity of $\omega_{\rm rot} = d\phi/dt = \omega$. For example, for $a = 18$ cm, the resonant frequency of the cavity would be $\omega = 6.3 \cdot 10^9$ rad/s ($f \approx 1$ GHz) and the rotating angular velocity of the wave would also be $d\phi/dt = \omega = 6.3 \cdot 10^9$ rad/s.

The magnetic field $H = \sqrt{H_\phi^2 + H_r^2}$ for the TM_{110} cavity, is shown in Fig. 5(b). It is this rotating magnetic field that is commonly utilized in the transverse modulation of particle beams (gyrocon, magnicon). Near the axis ($k_c r \ll 1$), $J_1(k_c r) \approx k_c r/2$ and $J_2(k_c r) \approx ((k_c r)^2/8)$. Letting $H_x = H_r \cos\phi - H_\phi \sin\phi$ and $H_y = H_r \sin\phi + H_\phi \cos\phi$, the magnetic field in rectangular coordinates can be expressed as

$$H_x = \frac{E_0}{(2c\mu)} \cos\omega t \qquad H_y = \frac{E_0}{(2c\mu)} \sin\omega t.$$

At any *point on-axis*, the magnetic vector $\boldsymbol{H}$ is constant in amplitude, but rotates in the ϕ direction at the RF angular frequency ω. The particles entering the cavity will then encounter this constant amplitude magnetic field rotating in the ϕ direction. Because the $\boldsymbol{H}$ field is constant, all particles (of velocity v) will be deflected by the same constant force $e\mu(v \times \boldsymbol{H})$; however, because the $\boldsymbol{H}$ field rotates in time, particles entering the cavity at different times will be deflected in different directions. Thus, upon exiting the cavity, the particles form a spiraling beam shown in Fig. 6.

VI. Conclusions

Rotating waves are neither standing waves nor traveling waves but have the field profile similar to a ϕ directed traveling wave and the discrete resonant frequencies of standing waves. An analysis of electromagnetic rotating waves, including their field dependence on standing waves, frequencies, energy, and power, has been presented in this paper for cylindrical cavities. The concepts of angular momentum, resonant frequencies, and electromagnetic fields in different types of rotating wave modes have been studied. A number of interesting and unique properties of rotating waves were discussed, including their constant electric and magnetic field energies. We mentioned a range of current uses for rotating waves in this paper; however, it is hoped that rotating electromagnetic waves, once better understood, may be utilized in an even wider range of applications.

References

[1] D. K. Cheng, *Field and Wave Electromagnetics*, 2nd ed. Reading, MA: Addison-Wesley, 1983, p. 647.
[2] V. L. Granatstein and I. A. Alexeff, *High Power Microwave Sources*. Boston, MA: Artech House, 1987, p. 120.
[3] G. I. Budker *et al.*, U.S. Patent 3,885,193 (1975).
[4] M. M> Karlirner, "The magnicon—An advanced version of the gyrocon," in *Nuclear Inst. and Meth. Phys. Reser.*, A269, Amsterdam, The Netherlands: North-Holland, 1988.
[5] W. M. Manheimer, "Theory and conceptual design of a high-power highly efficient magnicon at 10 and 20 GHz," *IEEE Trans. Plasma Sci.*, vol. 18, pp. 632–645, June 1990.
[6] P. H. Ceperley, "Rotating waves," *Amer. J. Physics.*, Dec. 1992.
[7] ——, "Split mode traveling wave ring resonator," U.S. Patent 4,686,407, 1987.
[8] T. Koryuishii, *Microwave Engineering, 2nd ed.* New York: Harcourt Brace Jovanovich, 1989, pp. 133–134.
[9] F. F. Chen, *Introduction to Plasma Physics and Controlled Fusion*. New York: Plenum, 1990, p. 20.
[10] W. C. Elmore and M. A. Heald, *Physics of Waves*. New York: Dover, 1985, p. 260.
[11] J. R. Pierce, *Almost All About Waves*. Cambridge, MA: MIT Press, 1974, p. 88.
[12] J. D. Jackson, *Classical Electrodynamics*. New York: Wiley, 1966, pp. 546–550, 65, 64.
[13] P. B. Visscher, *Fields and Electrodynamics*. New York: Wiley, 1988, pp. 222–224.
[14] S. Liao, *Microwave Devices and Circuits*. Englewood Cliffs, NJ: Prentice-Hall, 1985, pp. 137–138.
[15] M. Abramowitz and I. A. Stegun, *Handbook of Mathematical Functions*. New York: Dover, 1964, p. 358, 361, 437.
[16] S. Ramo and J. R. Whinnery, *Fields and Waves in Communication Electronics*, 2nd ed. New York: Wiley, 1984, pp. 138, 244.
[17] J. E. Velazco, Ph.D. dissertation.
[18] R. E. Collin, *Foundations for Microwave Engineering*. New York: McGraw-Hill, 1966, p. 190.

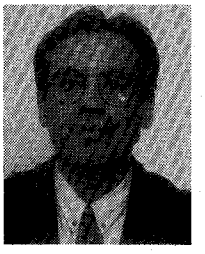

Jose E. Velazco (S'89–M'90) was born in Arequipa, Peru, on September 17, 1960. He received the B.S. degree in engineering from the Naval Academy in Peru in 1982, and the M.S. degree in electrical engineering from George Mason University, Fairfax, VA, in 1990.

In 1989 he joined the Microwave Research Laboratory at George Mason University as a Research Assistant, where he has been involved in the design, construction, and experimental investigation of a high-power transverse-modulated klystron. He is currently a Ph.D. degree candidate in the School of Information Technology and Engineering at George Mason University. His research interests include the study of circularly polarized electromagnetic fields theory and its application to the generation of high-power microwave radiation.

Mr. Velazco is a member of Eta Kappa Nu and the American Physical Society.

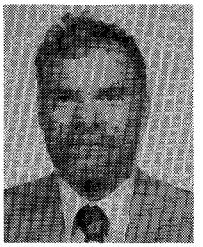

Peter H. Ceperley was born in Charleston, WV, on September 5, 1945. He received the B.S. degree from the University of Michigan and the Ph.D. degree from Stanford University, specializing in design of superconducting particle accelerators in 1967 and 1973, respectively.

He is currently on the Faculty at George Mason University, Fairfax, VA, in both the Physics Department and the Electrical and Computer Engineering Department. He does research on waves of various kinds, including those in thermoacoustic devices (which use intense acoustic waves to pump heat).